Received: 7 February 2020 | Accepted: 9 June 2020
DOI: 10.1002/hyp.13847

WILEY

RESEARCH ARTICLE

Characterising groundwater–surface water interactions in idealised ephemeral stream systems

Edisson A. Quichimbo[1] | Michael B. Singer[1,2,3] | Mark O. Cuthbert[1,2,4]

[1]School of Earth and Ocean Sciences, Cardiff University, Cardiff, UK

[2]Water Research Institute, Cardiff University, Cardiff, UK

[3]Earth Research Institute, University of California Santa Barbara, Santa Barbara, California

[4]Connected Waters Initiative Research Centre, University of New South Wales, Kensington, New South Wales, Australia

Correspondence
Edisson A. Quichimbo, School of Earth and Ocean Sciences, Cardiff University, Cardiff, UK.
Email: quichimbomiguitamaea@cardiff.ac.uk

Funding information
Cardiff University, Grant/Award Number: Vice-Chancellor's International Scholarship for Re

Abstract

Transmission losses from the beds of ephemeral streams are thought to be a widespread mechanism of groundwater recharge in arid and semi-arid regions and support a range of dryland hydro-ecology. Dryland areas cover ~40% of the Earth's land surface and groundwater resources are often the main source of freshwater. It is commonly assumed that where an unsaturated zone exists beneath a stream, the interaction between surface water and groundwater is unidirectional and that groundwater does not exert a significant feedback on transmission losses. To test this assumption, we conducted a series of numerical model experiments using idealised two-dimensional channel-transects to assess the sensitivity and degree of interaction between surface and groundwater for typical dryland ephemeral stream geometries, hydraulic properties and flow regimes. We broaden the use of the term 'stream–aquifer interactions' to refer not just to fluxes and water exchange but also to include the ways in which the stream and aquifer have a hydraulic effect on one another. Our results indicate that deep water tables, less frequent streamflow events and/or highly permeable sediments tend to result in limited bi-directional hydraulic interaction between the stream and the underlying groundwater which, in turn, results in high amounts of infiltration. With shallower initial depth to the water table, higher streamflow frequency and/or lower bed permeability, greater 'negative' hydraulic feedback from the groundwater occurs which in turn results in lower amounts of infiltration. Streambed losses eventually reach a constant rate as initial water table depths increase, but only at depths of 10s of metres in some of the cases studied. Our results highlight that bi-directional stream–aquifer hydraulic interactions in ephemeral streams may be more widespread than is commonly assumed. We conclude that groundwater and surface water should be considered as connected systems for water resource management unless there is clear evidence to the contrary.

KEYWORDS
dryland hydrology, ephemeral streams, groundwater recharge, stream–aquifer interactions

1 | INTRODUCTION

Loss of water through the streambeds of ephemeral streams is thought to be a key pathway of aquifer recharge in arid and semi-arid dryland regions (Costa, Bronstert, & de Araújo, 2012; Cuthbert et al., 2019; Keppel & Renard, 1962; Lerner, Issar, & Simmers, 1990; McCallum, Andersen, Giambastiani, Kelly, & Ian Acworth, 2013; Qin et al., 2012; Renard & Keppel, 1966; Wang, Pozdniakov, & Vasilevskiy, 2017; Wang, Yu, Pozdniakov, Grinevsky, & Liu, 2014; Wheater, Sorooshian, & Sharma, 2008). Such regions sustain a high population, more than 38% of the global population (GLP, 2005; Reynolds et al., 2007), who mostly rely on groundwater resources as their primary source of freshwater (Dai, 2012; Feng & Fu, 2013; Huang, Yu, Guan, Wang, & Guo, 2015; IPCC, 2013; Trenberth et al., 2013). For this reason, understanding the mechanisms of recharge from ephemeral streams is of critical importance for sustainable management of water resources in dryland regions (Gleeson, Cuthbert, Ferguson, & Perrone, 2020). Key to developing improved understanding of such dryland processes is a better appreciation of the degree and extent of interactions between surface water and groundwater (SW–GW) within ephemeral stream systems. Furthermore, improved understanding of the moisture dynamics below and around ephemeral streams would enable a better characterisation of water availability to dryland vegetation (Sargeant & Singer, 2016; Snyder & Williams, 2000) and thus climate–groundwater interactions (Cuthbert et al., 2019), as well as biogeochemical processing of key nutrients and contaminants within the short-lived hyporheic zone (Belnap, Welter, Grimm, Barger, & Ludwig, 2005; Meixner et al., 2007; Singer, Harrison, Donovan, Blum, & Marvin-DiPasquale, 2016; Valett, Fisher, & Stanley, 1990).

However, ephemeral streams are under-represented in existing hydrological research into SW–GW interactions, with much greater emphasis being placed on interactions under perennial streamflow conditions (Jarihani, Larsen, Callow, McVicar, & Johansen, 2015). Nevertheless, insights from studies of perennial losing streams can be useful in informing a deeper conceptual understanding of ephemeral streams. For example, the steady-state loss of water from a perennial stream has previously been characterised as follows (Brunner, Cook, & Simmons, 2009; Brunner, Simmons, & Cook, 2009; Fox & Durnford, 2003; Xian, Jin, Liu, & Si, 2017): (a) *connected* state, in which fully saturated conditions are developed in the region between the stream and the aquifer; (b) *transitional* state, characterised by a partially saturated zone between the stream and aquifer; and (c) *disconnected* state, in which an unsaturated zone occurs between the stream and the aquifer. For a connected state under steady conditions, the infiltration rate increases linearly with the water table depth, whereas for the disconnected state, the infiltration rate stays at its maximum value regardless of the water table depth, although theoretically, its behaviour is asymptotical. The transitional state is an intermediate state in which the relationship between the infiltration rate and the water table is non-linear. Under transient conditions, for connected streams, the infiltration rate is expected to vary gradually under changes in the river stage, whereas for disconnected streams the infiltration rate will immediately change, reaching a new steady state, after any change in the stream stage.

Despite this nomenclature becoming widespread in the literature, we note that, even during a so-called disconnected state, flow of water still occurs between the stream and the aquifer—there is no hydraulic disconnection between SW–GW in real terms. Rather, the term 'disconnected' simply refers to the fact that additional lowering of the water table cannot induce a greater loss from the stream for that particular set of conditions. The 'stream–aquifer' research community often use the term 'interaction' synonymously with 'exchange' of fluxes (Brunke & Gonser, 1997; Brunner, Cook, & Simmons, 2011; Winter, 1995). However, here we are using the term 'interaction' in a broader sense to encompass the ways in which the stream and aquifer have a hydraulic effect on one another. Thus, we consider that the hydraulic interaction between surface and groundwater in the 'disconnected' state is still *uni-directional*, whereas in the 'connected' state there can be feedback from the groundwater to the surface water and thus the hydraulic interaction can be said to be *bi-directional*. We also note that the state of the system may change through time (see, e.g., Rau et al., 2017), a further reason that categorising SW–GW interactions as connected or disconnected may be misleading.

An important characteristic of SW–GW interactions that has been also shown in previous studies is the development of an inverted water table (IWT) (Peterson & Wilson, 1988; Wang et al., 2016; Xian et al., 2017; Xie, Cook, Brunner, Irvine, & Simmons, 2014). The IWT is defined as the saturated zone immediately underneath the stream where the total pressure is equal to atmospheric pressure (i.e., pressure head equals zero). However, owing to a lack of field observations, the development of the IWT has only been tested using laboratory and numerical experiments (Wang et al., 2016). Such research shows that, under steady-state conditions, the IWT could develop inside the streambed for homogeneous materials and stream stages smaller than the streambed thickness (Wang et al., 2016), whereas for thin streambeds it may extend well below the bottom of the streambed (Brunner et al., 2011; Brunner, Cook, & Simmons, 2009; Brunner, Simmons, & Cook, 2009; Fox & Durnford, 2003). Under changes in stream stage, for thin streambeds, the extension of the IWT may increase or decrease immediately below the streambed, whereas for thicker streambeds the development of the IWT will gradually increase its size for any change in stream stage (Xian et al., 2017). In ephemeral streams we anticipate that the development of the IWT should be controlled by factors such as the degree of saturation, initial water table depth, the magnitude, timing and sequencing of streamflow events and hydraulic properties, including anisotropy, of the streambed sediments. However, these factors have not yet been evaluated in the literature, despite recent advances in understanding the nature of groundwater mounding beneath ephemeral streams (Cuthbert et al., 2016).

In addition to a lack of fundamental research on the general understanding of SW–GW interactions in ephemeral streams at small scales, its importance at larger scales has also been neglected (Alkama et al., 2010; Decharme, Alkama, Douville, Becker, & Cazenave, 2010; Döll, Douville, Güntner, Schmied, & Wada, 2016; van Beek & Bierkens, 2009; Wada et al., 2010; Wada, Wisser, & Bierkens, 2014). In addition, previous work has not properly characterised ephemeral stream–aquifer interactions in a manner that enables them to be

incorporated into larger-scale hydrological or land surface models (Döll et al., 2016; Taylor et al., 2012) despite their recognised importance for generating focussed recharge.

Here, we first propose a general conceptual model for characterising the main factors that control SW–GW interactions in ephemeral streams and their role in affecting the water balance of arid and semiarid regions. These concepts are then tested using a series of numerical model simulations, enabling the quantitative evaluation of different scenarios of stream–aquifer interactions.

2 | A CONCEPTUAL MODEL OF EPHEMERAL STREAM–AQUIFER INTERACTIONS

Despite the paucity of research on ephemeral stream–aquifer interactions, existing hydrological theory can inform the likely range of controls on these interactions. We propose that the following factors will be most important in controlling the degree of bi-directional hydraulic interactions: water table depth, stream stage, hydrograph shape, time between events, channel shape, channel boundary permeability and water retention characteristics of the subsurface materials. All these factors may vary individually or in combination in real systems. For example, channel shape will impact the infiltrated volume by increasing or decreasing the wetted perimeter and, consequently, the rate of infiltration through the streambed. Streambed permeability will increase infiltration rates for high values of permeability and reducing it for low values. Flow duration and frequency affect the amount of water available ultimately available for infiltration, and the amount of water than can infiltrate will depend on the degree of saturation and the water table depth. To illustrate the general way in which interactions may occur, we can characterise two end-member responses for 'deep' and 'shallow' water table systems that depend on the variations between these parameters as shown in Figure 1.

In the case of a deep water table, the frequency of events will affect the degree of saturation based on the prevailing time of drainage between events and consequently, the rate at which the channel bed can infiltrate newly arrived water. The process of water flowing through a thick variably saturated zone is depicted in Figure 1a in a two-dimensional cross section. When the stream stage starts to rise the IWT starts to develop, at a growth rate and size that are controlled by the antecedent saturation and the hydraulic conductivity of the sediments. Under lower antecedent saturation, which occurs under long time periods between flood events, more water will infiltrate below the streambed due to higher hydraulic gradients. The rate of movement of the IWT will depend on the degree of saturation, and for lower values of saturation the IWT will move more slowly downwards. The movement of the IWT will also be affected by anisotropic characteristics of the sediments, which may favour increased horizontal spreading of water. At the end of the event, the IWT becomes separated from the streambed as it descends due to gravitational drainage. At the same time, it decreases in size (areas decrease from t1 to t5 in Figure 1a) due to the losses associated with the spreading of water due to capillary forces. No influence of the water table depth is expected during the advance of the IWT for this case of a deep water table, and the rate of IWT movement is only a function of the saturation state of the sediment surrounding and below the channel.

For the case of a shallow groundwater system, the frequency of streamflow events combined with the antecedent water table depth will influence the infiltration rate. This process is shown in Figure 1b. Under this scenario, as the IWT develops within the thin variably saturated zone it rapidly interacts with the shallow water table creating a continuous zone of saturation beneath the stream; the hydraulic gradient is thus reduced and consequently the infiltration rate declines.

For both shallow and deep water tables, the change in saturation within the material surrounding and below the channel under different pressure heads will depend on their hydraulic and water retention properties (hydraulic conductivity and soil moisture retention curve).

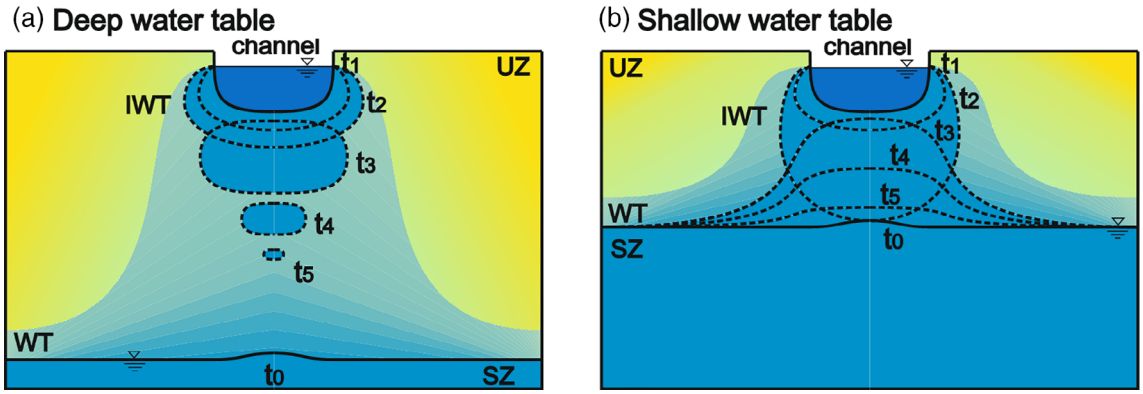

FIGURE 1 Conceptual process model of interactions between ephemeral streams and an underlying homogeneous aquifer for (a) deep and (b) shallow water tables. Dashed lines represent the evolution of the inverted water table (IWT) and the water table mound at time t_i during and after a streamflow event. The hypothetical shape and size of the IWT depend on the magnitude, shape and duration of the streamflow hydrograph and the antecedent conditions of saturation (inherited from the previous dry period), as well as hydraulic and soil moisture retention properties of the sediments

In this article, we seek to test and generalise this conceptual understanding via idealised numerical modelling, which enables quantification and insight into a poorly understood process that is very common in drylands.

3 | METHODS

3.1 | Numerical modelling

The purpose of the numerical modelling was to quantify the influence of key factors that control transient infiltration rates from ephemeral streams. A set of scenarios was developed to simulate the transient characteristics of the infiltration process under variations in: (a) magnitude/duration of streamflow events; (b) frequency of the events (and inter-arrival times); (c) initial water table depth; (d) hydraulic properties including soil moisture retention properties of the homogeneous material underlying the channel; and (e) the channel geometry. Our intention here is not to provide a comprehensive analysis across all possible dryland stream configurations and parameter sets. Rather we seek to demonstrate the general behaviour of ephemeral steam-aquifer interactions by quantitatively testing our conceptual model with a focus on developing a process-based understanding of such systems.

3.1.1 | Model geometry

The model was defined as a 2D cross sectional block containing a rectangular ephemeral channel, and a broad homogeneous aquifer (unconfined and variably saturated) with a water table within it. This configuration is broadly representative of ephemeral streams of dryland regions, which typically express as relatively simple geometrical shapes (Singer & Michaelides, 2014; Sutfin, Shaw, Wohl, & Cooper, 2014). A homogenous aquifer with a cross-section of 100 m width and 60 m depth was used in which processes are modelled within a 'half-space' (Figure 2). The width of the model domain was located at a sufficient distance from the stream to avoid high variations of pressure head close to the boundaries. The width of the stream, which can greatly vary in ephemeral streams, was chosen to be 12 m, which broadly corresponds to the dimensions of an incised alluvial stream located in a piedmont or a lowland zone of studied arid or semiarid regions (Jaeger, Sutfin, Tooth, Michaelides, & Singer, 2017).

3.1.2 | Governing equations and numerical methods

Flow under unsaturated conditions can be described by the following equation (Richards, 1931):

$$(C_m + S_e S)\frac{\partial H_p}{\partial t} + \nabla\cdot(-Kk_r(\nabla H_p + \nabla z)) = Q_m \quad (1)$$

where H_p is the pressure head [L], K is the saturated hydraulic conductivity [LT^{-1}], k_r is the relative permeability [–], Q_m is a fluid source term [T^{-1}], z is the vertical elevation [L], S is the storage coefficient [L^{-1}], t is time [T], ∇ is the gradient operator, S_e [–] is the effective saturation estimated by:

$$S_e = \frac{\theta - \theta_r}{\theta_s - \theta_r} \quad (2)$$

where θ_s and θ_r represent the saturated and residual liquid volume fraction, respectively.

θ is described by using the van Genuchten soil moisture retention equation (van Genuchten, 1980):

$$\theta = \begin{cases} \theta_r + \dfrac{\theta_s - \theta_r}{(1 + |\alpha H_p|^n)^m} & H_p < 0 \\ \theta_s & H_p \geq 0 \end{cases} \quad (3)$$

where α [L^{-1}], n [–] and m [–] are empirical parameters, with m equal to $1 - 1/n$.

Relative permeability k_r is also estimated by the van Genuchten method in the following way:

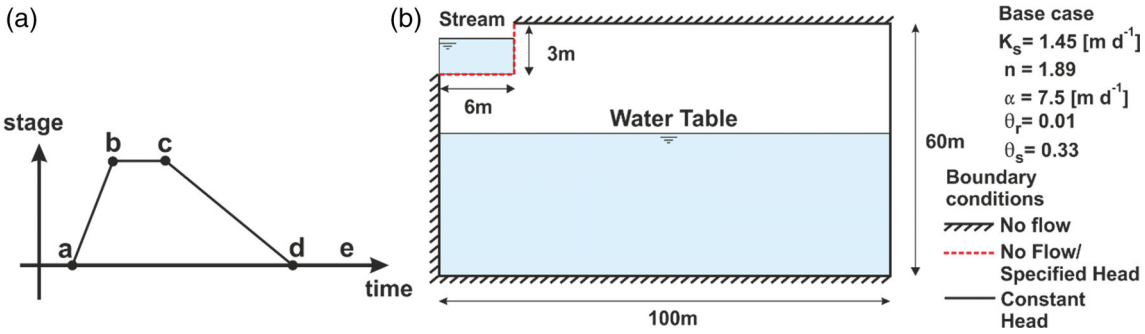

FIGURE 2 (a) Shape of the flow event is implemented as a specified head boundary condition at the stream base and sides. Before and after the flow event in the channel, the boundary condition switches to become 'no flow'; (b) cross section of the idealised transect considered in the numerical model, including a list of the boundary conditions and parameters of the base case model

$$k_r = \begin{cases} S_e^l \left[1 - \left(1 - S_e^{\frac{1}{m}} \right) \right] & H_p < 0 \\ 1 & H_p \geq 0 \end{cases} \quad (4)$$

The specific moisture capacity C_m [L^{-1}] is defined by the following equation:

$$C_m = \begin{cases} \frac{\alpha m}{1-m} \left[(\theta_s - \theta_r) S_e^{\frac{1}{m}} \left(1 - S_e^{\frac{1}{m}} \right) \right] & H_p < 0 \\ 1 & H_p \geq 0 \end{cases} \quad (5)$$

We chose to use COMSOL V5.1 Multiphysics for the numerical model in order to have the necessary flexibility in the applied equations and boundary conditions.

3.1.3 | Boundary conditions

COMSOL allowed us to define appropriate boundary conditions to represent the switch between ponded and dry channel conditions necessary to simulate ephemeral flows. Since COMSOL does not consider explicitly surface–subsurface interactions under saturation excess, this condition was implemented by assuming a continuity pressure and flux at the wetted perimeter of the channel. This was specified by using a Cauchy boundary condition (Chui & Freyberg, 2009; Jazayeri-Shoushtari, Nielsen, Cartwright, & Perrochet, 2015) to switch between Dirichlet and Neumann boundary conditions, representing pressure head and flux conditions, respectively, by following a similar approach described by Chui and Freyberg (2009):

$$K\nabla(H_p + z) = R(H_r - H) \quad (6)$$

where: $H_r = z + y$ represents the hydraulic head in the channel, and $H = z + H_p$ represents the hydraulic head in the streambed, y is the stream stage [L], and R is a conductance term [L^{-1}]. Values of R in Equation (6) should be large enough in order to guarantee a pressure continuity at the streambed and to keep at the same time the pressure head similar to the stream stage at the bottom of the channel. In the present simulation, a value of 1,000 d^{-1} for R was specified in order to assure the accuracy and convergence of the model results in acceptable simulation times.

In order to simulate ephemeral channel conditions, the parameter R was switched to zero when the stream stage was zero, creating a no-flow boundary condition. This switching was applied gradually over a period of 2 hours prior and after the event by using a smoothing function in order to enable convergence of the model during the large changes in hydraulic gradient that result (Chui & Freyberg, 2009; Chui, Low, & Liong, 2011).

In order to define the size and distribution of the finite element model mesh, various geometrical distributions were analysed in order to ensure the accuracy and convergence of the results. As a result, a triangular mesh was specified for the entire model domain, in which the size of the elements varies between 0.05 and 1.0 m, according to the characteristics of the flow and the balance between the model accuracy and efficiency. Elements with a minimum size of 0.05 m were specified in the region below the stream (Figure 2). The mesh was also refined in the region located between the water table and the streambed as well as above the water table. These refined regions allowed for a better representation of the highly non-linear behaviour of the unsaturated zone at the region corresponding to the capillary fringe.

The solution for the numerical model was obtained using the numerical solver MUMPS (MUltifrontal Massively Parallel sparse direct Solver) in COMSOL v5.1. MUMPS, which is based on the lower–upper decomposition, used an adaptive time step with a minimum time step of 0.001 d, although the time step for the model output was specified as 1 hour in order to optimise computational resources.

3.1.4 | Initial conditions

Choice of initial conditions in ephemeral streams is non-trivial due to complex antecedent moisture conditions implicit in such systems. Two options for initial conditions often used in unsaturated zone models are either a hydrostatic initial state of the water table and unsaturated zone or a periodic steady state for a specific dry period length. However, both of these can be unrealistic considering the typically highly variable frequency of flow events in ephemeral systems. Thus, we implemented a compromise between these end members as follows. First, a steady-state condition for a small stream stage corresponding to 0.5 cm was specified in order to raise the moisture state of the unsaturated zone above the unrealistically dry conditions that hydrostatic conditions would imply. Second, using this initial steady-state condition the stream stage was then set to zero in order to let the sediment drain and to allow the dissipation of groundwater mound for a period of approximately a year (360 days) of no flow. Third, at the end of this no flow period, a pair of identical flow events was modelled using the various types of flow event described below, separated in time by a dry period whose duration was also varied as described below. The second event of the pair was then analysed and included in the results presented in the following sections.

3.2 | Base case scenario and sensitivity analysis

A base case model was defined with a K of 1.45 m day^{-1}, which corresponds to sandy loam sediments (Carsel & Parrish, 1988). This is consistent with the permeability of a sandy streambed typical of ephemeral streams characterised as high-energy environments, due to high flow velocities that can reduce the chance of the deposition of fine sediments on the bottom of stream (Peterson & Wilson, 1988; Xie et al., 2014). While it is recognised that clogging layers can be deposited as ephemeral flows abate, they are also often scoured out during the first stages of the next event (Lerner et al., 1990). Given

the objectives of the modelling to determine behaviour in a homogeneous system, this complication is out of scope of this article but will be included in future work. Unsaturated soil parameters for the van Genuchten soil water-retention curve of a sandy loam sediment were assigned as 7.5 m^{-1} and 1.89 for α and *n*, respectively, and 0.01 and 0.33 for residual, θ_r, and saturated, θ_{sat}, moisture water content, respectively (Carsel & Parrish, 1988). A pair of trapezoidal, 7-day flow events were then simulated, in which the rising limb lasted 1 day, the peak was represented as a flat period of 1 day, and the falling limb comprises 5 days. The dry period between the pair of events was 10 days for the base case model.

Ephemeral streamflow events can show a huge variation in hydrograph shape, return period and duration. In small ephemeral streams, streamflow shape is characterised by a rapid increase and decrease of the stream stage (Costigan et al., 2017; Malmon, Reneau, & Dunne, 2004). However, the peaks can decrease slowly for longer ephemeral flood events (Dahan et al., 2008; Vivoni, Bowman, Wyckoff, Jakubowski, & Richards, 2006). Streamflow durations can vary from several hours up to several days (Cataldo, Behr, Montalto, & Pierce, 2004; Constantz & Thomas, 1997; Costigan et al., 2017; Jarihani et al., 2015; Knighton & Nanson, 1994; Wheater et al., 2008) or even weeks (Rau et al., 2017). Therefore, variations from the base case were simulated in order to assess the sensitivity of the stream–aquifer interactions to the aspects hypothesised to be important (see conceptual model description, Section 2) as follows: streamflow duration, dry period length between flow events and hydraulic properties.

3.3 | Streamflow duration and water table depth

The shape of the event hydrograph was varied by changing the total duration of the event from 7 to 16 days. The rising and falling limb of the hydrograph were kept the same as the base case scenario (i.e., 1 and 5 days for the rising and falling limb, respectively) but the duration of the peak of the event was varied with values of 1 (base case), 5 and 10 days.

3.4 | Length of dry period between streamflow events

The influence of the dry conditions is evaluated by two streamflow events separated by a specific period of time. Time periods between events allow the drainage of water from the unsaturated zone and the dissipation of the water table mound after a streamflow event occurs, these conditions are reflected in the degree of saturation and water table depth and they become the initial condition for the next event.

Duration of the dry period shows great variability in real ephemeral streams (Costigan et al., 2017), in part due to the high spatiotemporal variability in runoff-generating rainfall events (Michaelides, Hollings, Singer, Nichols, & Nearing, 2018; Singer & Michaelides, 2017). Therefore, we have used a range of 10–360 days for the duration of the dry period in order to include seasonal variations (Table 1). The analysed event corresponded to an event peak of 5-day duration event for the simulations.

3.5 | Soil hydraulic and water retention properties

The characteristics considered in the sensitivity analysis were: (a) hydraulic conductivity, (b) water retention curve and (c) storage capacity. These were evaluated separately and are summarised in Table 1. Values of *K* were varied between 1.0 and 2.0 m d^{-1} in addition to the base case value of 1.45 m d^{-1}. For the water retention curve, its shape was varied by changing the α and *n* parameters (Table 1). Higher values of α and *n* correspond to coarser material with higher content of sand while low values of these parameters correspond to finer material with higher clay content. Finally, the available storage capacity of the material ($\theta_s - \theta_r$) was varied by increasing and decreasing the saturated water content by ±10%.

3.6 | Transmissivity

The influence of aquifer transmissivity was evaluated by increasing and reducing the height of the model domain by 10 m while keeping the *K* value constant.

3.7 | Channel cross-section shape and channel width

Channel cross-section was evaluated by changing the channel width in relation to the base case scenario. For a channel width larger than the base case scenario, the model domain was also increased in order to reduce the influence of lateral boundary conditions. Since it is intuitive that the increase in channel width increases the total infiltration, the infiltration per unit length flowing through the streambed was used for comparative analysis. Channel cross section shape was also considered by simulating and comparing results for rectangular, triangular and trapezoidal shapes. For the latter two cross sections, a slope of 1:1 was specified for the channel banks.

3.8 | Combinations of parameters used in sensitivity simulations

All variations of the above parameter variations where carried out in combination with variations in initial water table depth values of: 1, 3, 5, 10, 15, 20 m below the streambed (Table 1). In addition, the length of dry period and event peak duration were also varied in combination. (Table 1).

TABLE 1 Model scenarios and number of events per scenario

Parameter being varied	Range of variation	Other parameters that were varied in combination (number of combined simulations in brackets)
Length of dry period between streamflow events	10 days (base case) 30 days 60 days 90 days 150 days 360 days	Water table depth (36)
Event peak duration	1 day (base case) 5 days 10 days	Water table depth Dry period (72)
Saturated hydraulic conductivity, K	1 m d^{-1} 1.45 m d^{-1} (base case) 2 m d^{-1}	Water table depth Dry period (72)
Soil hydraulic (van Genuchten) parameters, α and n	Coarse material: α = 10.4 m^{-1}; n = 2.28 Base case: α = 7.5 m^{-1}; n = 1.89 Fine material: α = 3.6 m^{-1}; n = 1.56	Water table depth (12)
Transmissivity	Aquifer thickness of 60 m (base case) Increase of 10 m of the aquifer thickness Decrease of 10 m of the aquifer thickness	Water table depth (12)
Storage capacity	−10%: θ_r = 0.01, θ_{sat} = 0.300 Base case: θ_r = 0.01, θ_{sat} = 0.33 +10%: θ_r = 0.01, θ_{sat} = 0.373	Water table depth (12)
Cross section shape	Rectangular (base case) Triangular Trapezoidal	Water table depth (12)
Cross section width	1 m 2 m 6 m (base case) 12 m 24 m	Water table depth (24)
Total number of simulations		252

Note: Each analysed event corresponds to the second streamflow event for each event pair simulated (see section 3.1.2.). Scenarios of water table depths (× 6) were 1, 3, 5, 10, 15 and 20 m below stream bed. Dry period between events (× 6) modelled were 10, 30, 60, 90, 150 and 360 d. Total number of events are in parenthesis. Parameters for the base case scenario are α = 7.5 m^{-1}; K = 1.45 m d^{-1}; n = 1.89.

4 | RESULTS

4.1 | Conceptualising a single flow event in time and space

Based on the results of the numerical simulations, the hydraulic processes governing the loss of water from an ephemeral stream transect can be described as follows for a 3-day streamflow event with a 1-day peak (Figure 3, stage hydrograph shown in Figure 4). During a streamflow event occurring after a dry period of no flow in the stream (Figure 3a,f), as the stream stage starts to rise a saturated zone and IWT start to develop at the bottom of the channel (Figure 3b,g).

For deep water tables, an IWT forms by the time the streamflow hydrograph has reached its peak value. In this case, the hydraulic head at the bottom of the channel is equal to the stream stage (2 m) plus the elevation (57 m), as shown in Figure 3b. At the IWT, where the pressure head equals zero, the hydraulic head is equal to the elevation head and consequently intersects the gravity drainage line. Immediately below the IWT, the hydraulic head plots above the gravity drainage line indicating unsaturated conditions. In the deeper water table case, the zone of saturation below the streambed continues expanding during the event until the streamflow ceases (Figure 3c), after which the IWT starts to move downward until it disappears as a result of lateral spreading dominated by capillary forces and downward spreading dominated by gravity forces (Figure 3d). Much of the remaining water above the water table, which is temporally stored in pores, continues to move downward through the unsaturated profile until it eventually reaches the water table producing recharge (Figure 3e). Since this process is relatively slow, no significant groundwater mound develops underneath the stream as the lateral movement of water in the aquifer towards the lateral boundary keeps pace with the rate of recharge.

By contrast, for the case of an initially shallower water table, the IWT quickly expands downwards developing a fully saturated zone between the stream and the aquifer (Figure 3g). However, the water table drops below the channel once the stream event ceases (Figure 3i). In this case, lateral groundwater flow cannot keep pace with the rate of recharge during the event and a groundwater mound is created beneath the stream (Figure 3j). For shallow water tables, the pressure head and the infiltration rate at the peak of the event are similar to those within deep water table simulations. However, fully saturated conditions between the stream and the aquifer are reached faster after the onset of the event for shallow water tables (Figure 3g) as a result of the reduced storage capacity and a higher antecedent moisture content arising from the initial conditions. Hence, at later times the infiltration rates are lower for a shallow water table compared with the deeper water

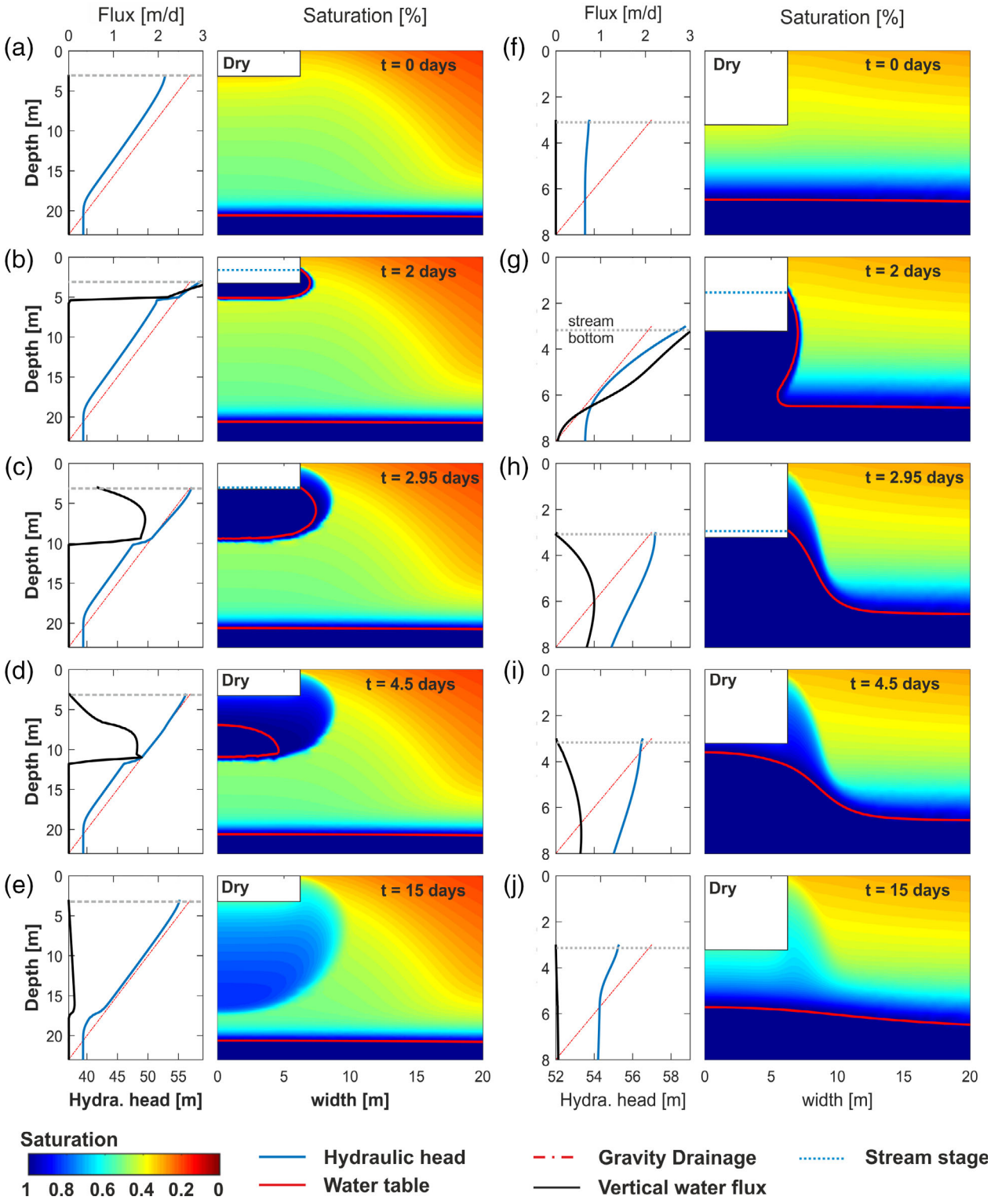

FIGURE 3 Variation of hydraulic head and vertical water flux at the centre of the stream, and saturation states for the cross section of the model domain for deep (a–e) and shallow (f–j) initial water table depths during the occurrence of a 3-day streamflow event (see stage hydrograph plotted in Figure 4a) which otherwise uses the base case scenario parameters and geometry (see Figure 2). Note that the vertical depth axes in (a–e) and (f–j) are different and zero depth corresponds to the base of the channel at an elevation of 57 m used in the calculation of hydraulic head

table case (Figure 3c,h), due to the lower hydraulic gradients produced by the quicker development of fully saturated conditions between stream and aquifer.

Figure 4 shows how vertical flow rate at the bottom of the channel and pressure head and saturation at 1.0 m below the bottom of the channel vary during the same streamflow event plotted in

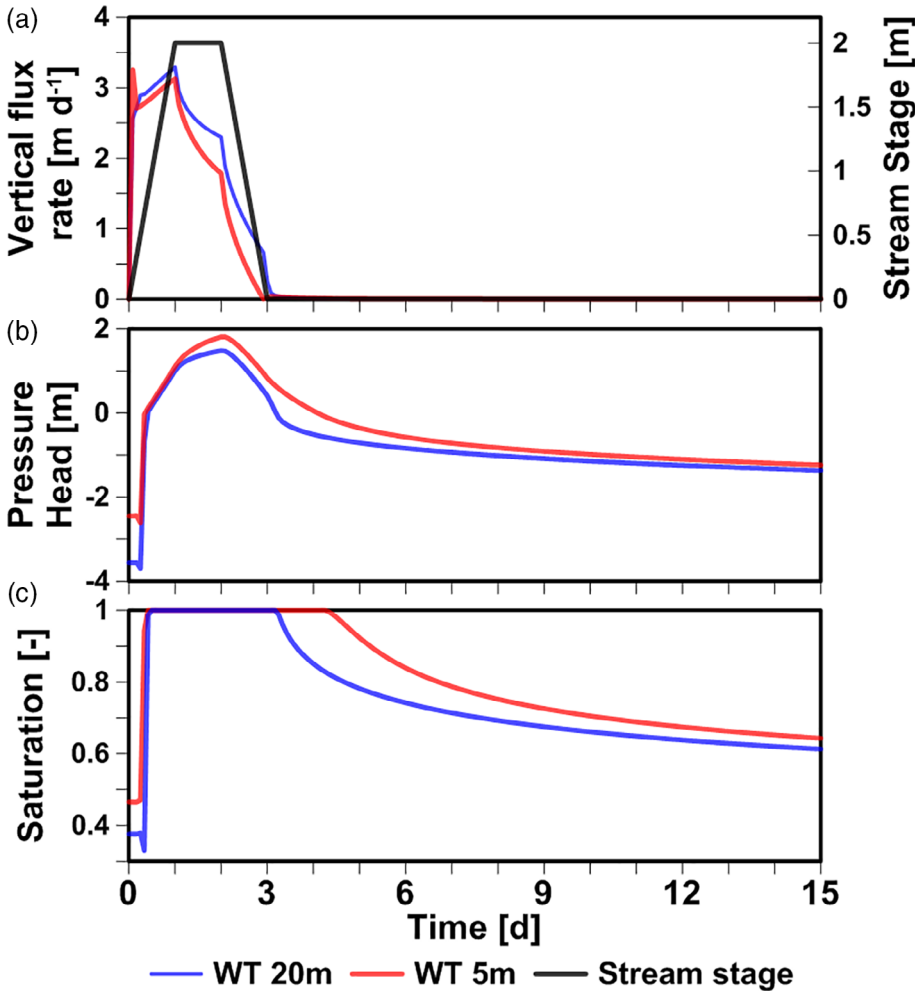

FIGURE 4 Temporal variation modelled at 1 m below the centre of stream (left side of model half-space) for the same scenarios of Figure 3: (a) infiltration rate, with stream stage shown for comparison on right-hand axis, (b) pressure head and (c) degree of saturation for deeper (20 m) and shallower (5 m) water tables (WT). Soil parameters correspond to the base case scenario (Figure 2)

Figure 3, for both the shallow and deeper water table cases. At the beginning of the event (t = 0 d), the infiltration rate suddenly increases as a result of the rapid change of the pressure head in the stream from zero to positive values, which in turn produces high hydraulic gradients driving flow as a result of the beginning of the development of a thin IWT. A step-decrease of the infiltration rate then follows, due to the rapidly declining hydraulic gradient at the streambed as the IWT continues to develop. As the stream stage rises the pressure head also rises but at a slightly slower rate, which in combination with the slower rate of development of the IWT results in the overall increase of the infiltration rate ($0 < t < 1$ d, Figure 4a).

When the stream stage reaches its peak (t = 1 d), the infiltration rate reaches its maximum values and suddenly declines due to the reduction of hydraulic gradient as a results of the continuous rise of the pressure head beneath the stream and development of the IWT ($1 \leq t < 2$ d, Figure 4a,b). The rate of rising of the pressure head for shallow water tables is larger than that for deep water tables due to the quicker feedback of the water table (Figure 4b). Finally, when the stream stage starts to fall (t = 2 d), the pressure head also decreases and becomes negative by the end of the flow event. This results in the decrease of the hydraulic gradient and consequently the reduction of the infiltration rate (Figure 4a).

4.2 | The influence of dry period duration between flow events and water table depth on streambed infiltration rates

As dry period duration between flow events varied, we found that total streambed infiltration increased with the length of dry periods, irrespective of water table depth (Figure 5a). The total volume of infiltration shows a particularly high range of variation for dry periods with a duration of less than ~35 days (Figure 5a). For longer dry period durations, the total volume of transmission losses approaches a constant value. As water table depth varied, we found that for water tables shallower than ~10 m, infiltrated volumes increase significantly with water table depth. For water tables deeper than 10 m, the variation of the total infiltrated volumes is relatively unaffected by any further increases in water table depth, although there are still small variations (<10%), associated with variations in dry period duration (Figure 5b).

These results are intuitive because for events occurring after short dry periods, we would expect the rate of decay of the degree of saturation to be higher after the event has ceased caused by the downward movement of the IWT (Figure 4c). For longer dry periods following an event, the rate of change in the degree of saturation

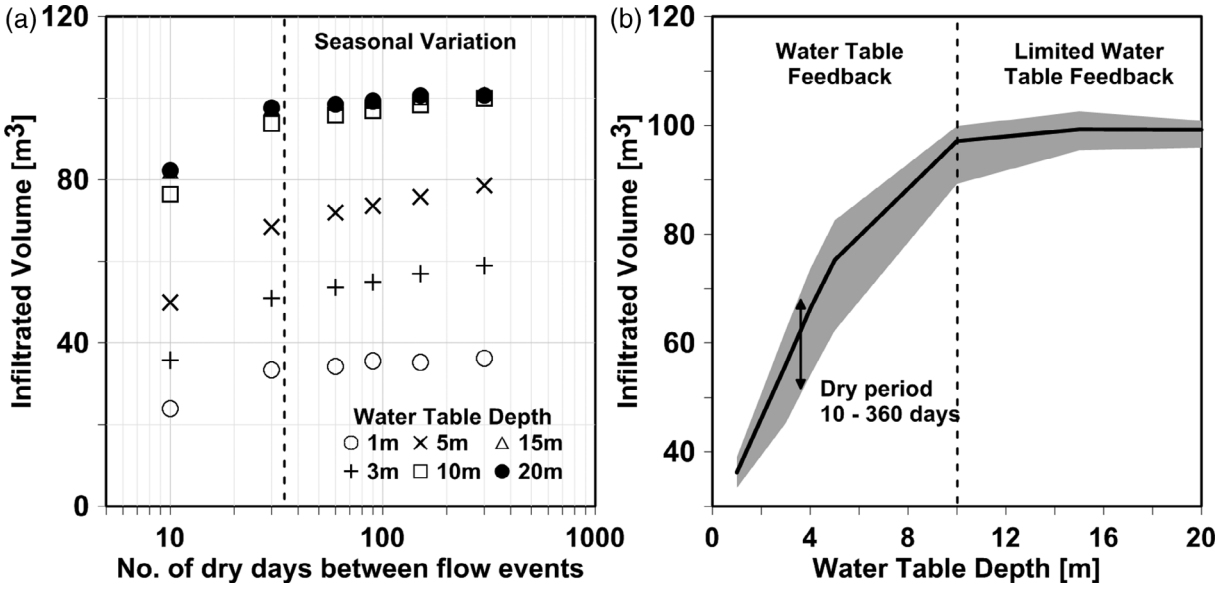

FIGURE 5 Variation of the total infiltrated volume into the streambed during one event against varying: (a) dry period durations between events (specified as the number of days with zero streamflow)—with different data series representing a different water table depth, dashed line represents the dry period at which the rate of variation of infiltrated water becomes log - linear, and (b) water table depths, with the variation due to different duration of dry periods indicated by the shaded area, dashed line represent the approximate apparent water table depth threshold

slows considerably, and becomes nearly constant (Figure 4c). This reduced variation of saturation states for long dry periods between events means that the infiltrated volume does not vary much when an event occurs, reaching an almost constant value depending on the depth of the water table (Figure 5a).

For shallow water tables of <3 m in our simulations, the range of variation of total infiltrated volume due to the length of dry period is also restricted, but in this case due to the rapid connection of the IWT with the water table and the influence of the capillary fringe (Figure 5a). The extension of the capillary fringe represents a region in which the degree of saturation reaches a constant value. Therefore, the initial conditions for a shallow water table will be similar for any dry period length, which in consequence will result in a similar volume of water losses for events, irrespective of dry period duration between events.

4.3 | The influence of streamflow duration

A summary of the simulation results used to test the influence of streamflow duration on total streambed infiltration volumes are shown in Figure 6. As expected, infiltrated volumes increase with the duration of the event. Variation in flow event duration shows that the maximum value of infiltrated volume is asymptotically reached later for longer streamflow durations and for deeper water table depths. For example, the increase in infiltrated volume reaches a steady value at water table depths of around 10, 15 and >20 m for 1-, 5- and 10-day-long flow events, respectively.

For shallow water tables, the increase of infiltration losses is limited due to the rise and lateral expansion of the groundwater

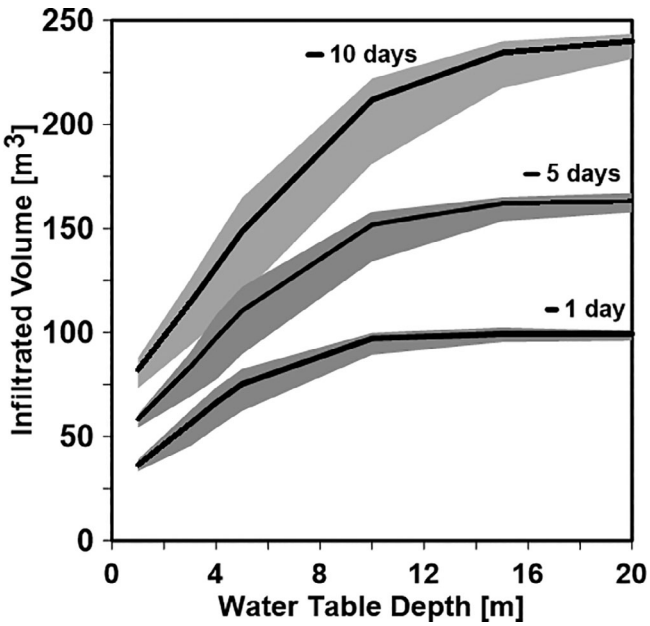

FIGURE 6 Variation of streambed infiltration volume during a single event as a function of the duration of the streamflow event, the length of dry period between events (shaded range in the style of Figure 5), and water table depth

mound below the stream, which quickly reduces the hydraulic gradient and regulates the infiltration rate (Figure 3i). For deep water tables, there is more pore-space available to enable continued lowering of the IWT which enables higher infiltration and, consequently, a larger increase in total infiltration volume (Figure 6). As the streamflow duration increases, the maximum depth at which this

feedback from the water table occurs is therefore also greater. Thus, the limit to the depth of eventual SW–GW bi-directional interactions may be 10s of metres in the scenarios simulated, but in principle even greater for other combinations of high permeability sediment and long flow durations.

4.4 | The influence of sediment properties

Overall our simulations showed that the total streambed infiltration volume per event increases as the sediment hydraulic conductivity increases (Figure 7a), the 'coarseness' of moisture retention curve increases (Figure 7b) or the amount of total pore space available increases (Figure 7c).

Total infiltration is particularly sensitive to changes in hydraulic conductivity because infiltration rate is proportional to the hydraulic conductivity and the hydraulic gradient. For a specific stream stage, the hydraulic head and consequently the hydraulic gradient remain similar. The opposite occurs for low values of hydraulic conductivity. However, when the shape of the moisture retention curve is changed, rates of infiltration also change due to changes in hydraulic gradients. Larger changes of hydraulic gradients are expected for coarser material, particularly at low degrees of saturation, due to the sharper change of pressure head in relation to water content. While total infiltration increases with increasing storage capacity as expected due to more pore space being available under partly saturated conditions, this effect is quite small. This suggests that the capacity for water to flow through the streambed and underlying sediments, rather than the absolute volume of storage available beneath the stream, is the primary control on the overall volume of streambed infiltration.

For the relatively high transmissivity values (68.2–95.7 $m^2\ d^{-1}$) considered in the analysis, our simulations (not shown) showed that the infiltration rates and water table depth thresholds are relatively insensitive to changes in this parameter. A small variation which varies from 5% for shallow water tables to 0.3% for the deeper water table was observed of the total infiltration rate in relation to the base case scenario due to the development and dissipation of the groundwater mound and its interaction with the IWT. For deep water tables, the interaction with the water table was limited, and consequently the variation of the total infiltration due to changes in transmissivity was negligible.

4.5 | The influence of geometrical characteristics of the stream channel

We found that infiltration through the streambed for both trapezoidal and rectangular channel geometries showed differences with higher values (6%, not shown) for the rectangular shape which are consistent with the shorter wetted perimeter in comparison with the trapezoidal shape that reduces the influence of lateral flow due to capillary flux during the advance of the IWT.

Since the triangular channel geometry does not have a 'streambed' as such (only a channel invert), for comparison of all three geometries tested, we compared infiltration rates just through the streams' banks. Figure 8 shows that the total bank-infiltrated volume increases substantially for both the triangular and trapezoidal shapes in comparison with the base case rectangular shape. The increase is also affected by the water table depth, although a threshold for maximum infiltration rates is still reached for deeper water tables for all cross-section shapes.

The increase of the bank-infiltrated volume for triangular and trapezoidal shapes is intuitive due to the increase of the wetted perimeter. The combination of both vertical and lateral flow driven by gravity and capillary forces plays an important role in total stream losses. The higher stream bank losses for a triangular cross section is explained by the smaller perimeter of the wetted front which makes

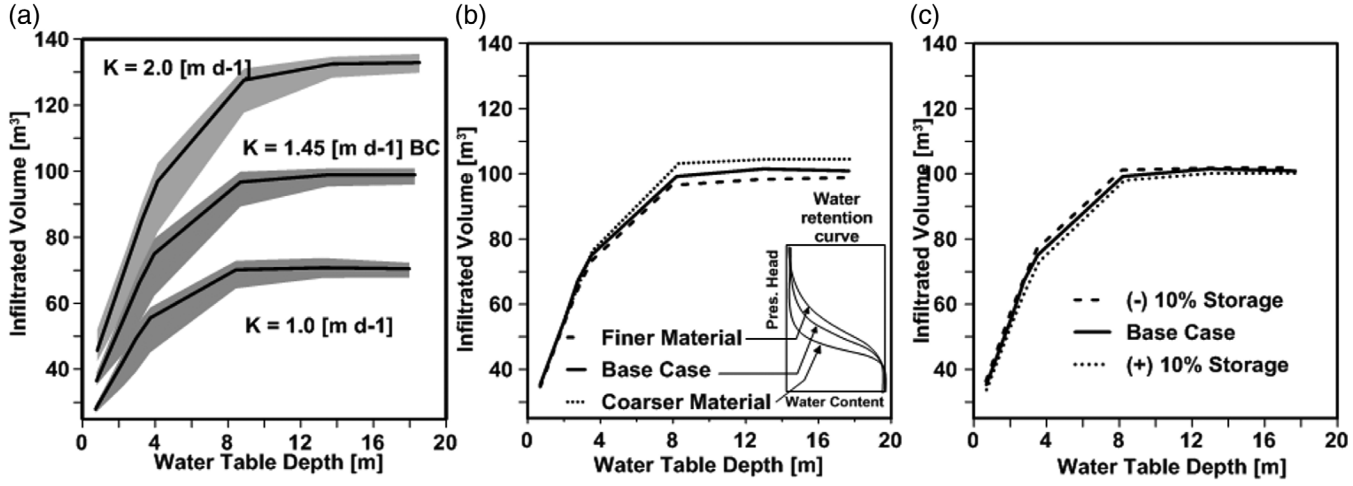

FIGURE 7 Variation of infiltrated volume in relation to water table depth for changes in the hydraulic properties: (a) hydraulic conductivity, shaded area indicates the range of variation for dry period duration between flow events of 10–360 days, (b) water retention curve shape and (c) variation of storage capacity; (b) and (c) correspond to a 7-day event occurring after a dry period of 360 days (see Table 1)

the combined horizontal–vertical flow reach higher values. For the trapezoidal shape, the base of the channel increases the perimeter of the overall wetted front affecting both the lateral flow due to capillary forces and the vertical flow which in turn results in less infiltration in comparison to the triangular shape. In the case of the rectangular channel, the small infiltrated volume at the banks is the result of the short wetted perimeter of the channel and the lower influence of lateral flow which in turn makes the vertical flow higher than the streambed flow of the trapezoidal shape section (Xian et al., 2017).

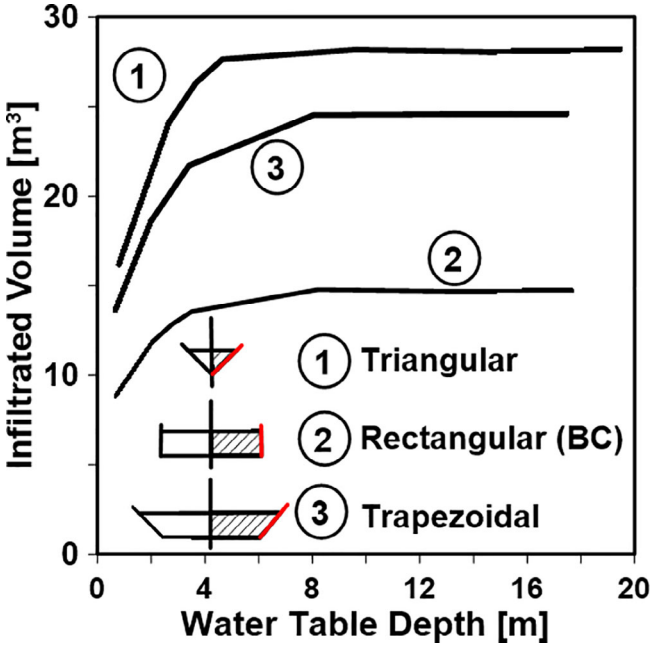

FIGURE 8 Variation of the infiltrated volume due to variations in the shape of the channel cross section for the flow event defined in the base case scenario. Plotted values correspond to water infiltrated only through the streambanks (red lines)

Figure 9 indicates that the infiltration per unit length varies for different combinations of changes in channel width and water table depth. For example, for wider channels, the infiltration per unit length receives feedback from the water table at deeper water tables whereas for narrow channels this interaction only occurs for shallower water tables (Figure 9a). The smaller degree of interaction with the water table for narrower channels is explained by the shorter wetted perimeter of the IWT which results in a rapid advance, at highest rates of infiltration, of the IWT. When the IWT reaches the water table, the development of a groundwater mound, which is also narrower, is more easily spread laterally due to the higher hydraulic gradient, resulting in less feedback to the infiltration rate. As the channel width increases, the interaction with the water table last longer due to the development of a bigger groundwater mound which reduces the hydraulic gradient and consequently the infiltration rate.

The variation of the infiltration rate through both the streambed and streambank shows a non-linear relation with the stream width. Figure 9b shows how the infiltration per unit length through the streambed changes from higher values for narrow channels to an almost constant value for wider channels. For shallow water tables, the streambed infiltration reaches a constant value for channels wider than 5 m, whereas for a deep water table of 20 m, the infiltration through the streambed only reaches a constant value for channel greater than 15 m. This result shows that lateral flow has greater influence in narrow channels than in wide channels. In addition, the infiltration rates through the streambanks increase as the water table depth increases as shown for the two end members plotted in Figure 9.

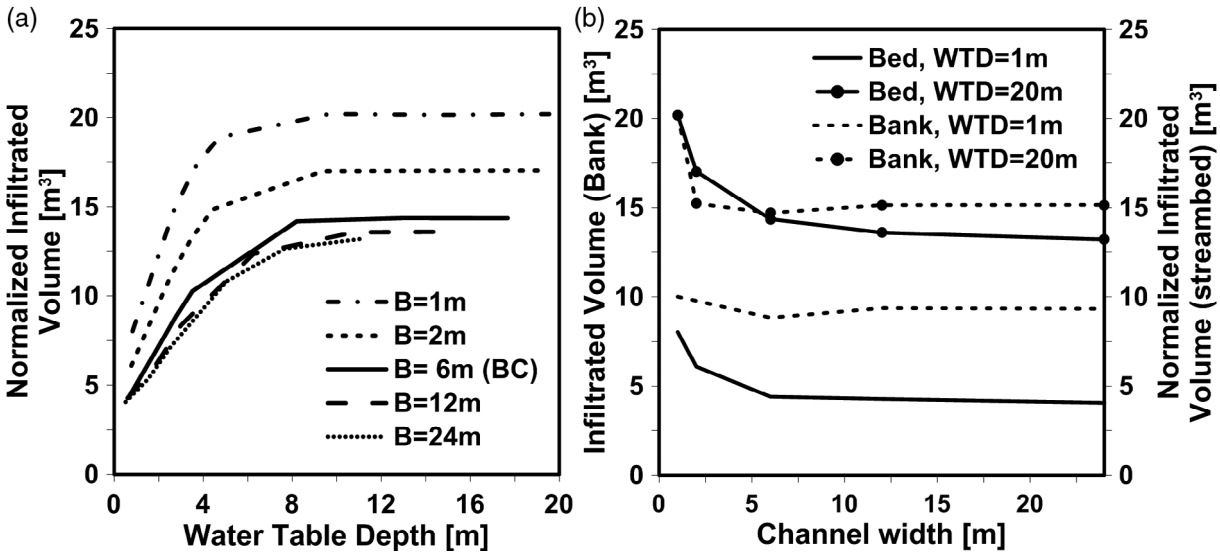

FIGURE 9 Channel width analysis: (a) Variation from the base case (BC) scenario of the infiltrated volume per unit length, for different stream channel widths (B) and water table depths; (b) variation of the volume infiltrated per metre width through the streambed (solid lines) and streambank (dashed lines) in relation to the channel width for a shallow and deep water table (WTD)

5 | DISCUSSION AND CONCLUSION

We set out to understand the process controls on transmission losses from idealised ephemeral stream beds in dryland environments. We first developed a conceptual model of factors that control infiltration through the variably saturated zone around, and below, an ephemeral streambed, and then quantified the relative importance of these factors using a suite of numerical model simulations. Specifically, we evaluated streamflow characteristics, time duration between streamflow events, water table depth, aquifer hydraulic properties and channel geometry.

For a given streamflow event, the initial saturation conditions characterised by the duration of the antecedent dry period, the hydraulic conductivity of the sediments, and the water table depth all provide strong controls of the infiltration rates lost from the stream. As expected from the conceptual model, deeper water tables combined with longer dry periods and higher hydraulic conductivity increase the amount of infiltrated water; the opposite occurs when these parameters decrease.

Our analyses of the variability of infiltration rates when the geometrical characteristics of the channel change, have important implications for hydrologic and land surface models, especially for large scale models where narrow channels are difficult to represent, which can result in the gross underestimation of infiltration rates. At smaller scales, the variation of infiltration rates through streambanks due to changes in the cross section will also impact the availability of water for biochemical processes occurring within the streambed.

Our simulations show that infiltration rates vary non-linearly with water table depth, although they become constant, dependent on the local conditions, when a threshold in the water table depth is reached. For a homogeneous aquifer with hydraulic properties corresponding to a sandy loam material, the threshold for a 7-day streamflow event (with a 1-day peak) is reached for water table depths greater than approximately 10 m. This threshold, beyond which bi-directional SW–GW interactions become limited, increases for longer events and can be 10s of metres in some of the scenarios tested. For different values of hydraulic conductivity, including anisotropy, a similar behaviour will be expected with a threshold that will vary depending on the exact combination of all components involved a particular situation.

In all these cases, the initial condition beneath the stream is one of partial saturation, and yet we demonstrate that feedback from the underlying groundwater is common during the simulated ephemeral streamflow events. Hence, we conclude that the paradigm of characterising streams as either 'connected' or 'disconnected' derived from studies of perennial streams (Brunner, Cook, & Simmons, 2009; Winter, Harvey, Franke, & Alley, 1998) is not applicable to ephemeral stream systems. We would, in fact, caution against the current practice of using the term 'disconnected' streams at all, in favour of referring to unidirectional or bi-directional SW–GW interactions, depending on the relative extent of feedback given by groundwater to stream losses.

The models presented here have been kept deliberately simple in order to quantify a first conceptual outline of the dynamics of SW–GW interactions in idealised ephemeral systems. Further work will also explore the influence of evapotranspiration, floodplain topography as well as anisotropy, heterogeneity and layering of sediments to test these concepts across a broader range of real-world hydrogeological contexts. Nevertheless, our results give an improved insight into the possible importance of bi-directional feedback between groundwater systems and ephemeral streams, and consequently to understanding of subsurface water availability to plants and potential for subsurface biogeochemical transformations. Such GW-SW interactions may be very widespread across dryland regions where water tables are typically within a few 10s of metres of the surface (Fan, Li, & Miguez-Macho, 2013). Oversimplified categorisation of ephemeral streams that assumes 'hydraulic disconnection' between SW and GW in dryland regions for water management purposes may be misleading since any increase or decrease in water table depth caused by natural or human activities could still affect the amount of recharge that the aquifer receives in many cases. Such 'capture' of additional recharge (Theis, 1940) is generally ignored for dryland regions (Bredehoeft, 1997, 2002; Bredehoeft, Papadopoulos, & Cooper, 1982). We suggest that there is a broad spectrum of channels present within dryland environments that function in a 'transitional', rather than a disconnected state. Since dryland groundwater supplies a significant proportion of the world's water for irrigated agriculture, and that the depletion of groundwater of such regions is a major global issue, more ongoing research into the potential feedbacks between SW and GW in these contexts in still needed.

ACKNOWLEDGMENTS

We gratefully acknowledge financial support from Cardiff University. MC gratefully acknowledges funding for an Independent Research Fellowship from the UK Natural Environment Research Council (NE/P017819/1). MBS acknowledges support from the US National Science Foundation Hydrologic Sciences (EAR no. 1700555), Geography and Spatial Sciences Program (BCS no. 1660490), and the US Department of Defense's Strategic Environmental Research and Development Program (no. RC18-C2-1006).

DATA AVAILABILITY STATEMENT

All data from the modeling used to generate the figures will be available via the Natural Environment Research Council's Environmental Information Data Centre (Terrestrial and freshwater).

ORCID

Edisson A. Quichimbo https://orcid.org/0000-0002-6811-3189

REFERENCES

1. Alkama, R., Decharme, B., Douville, H., Becker, M., Cazenave, A., Sheffield, J., … Le Moigne, P. (2010). Global evaluation of the ISBA-TRIP continental hydrological system. Part I: Comparison to GRACE terrestrial water storage estimates and in situ river discharges. *Journal of Hydrometeorology*, *11*, 583–600. https://doi.org/10.1175/2010JHM1211.1
2. Belnap, J., Welter, J. R., Grimm, N. B., Barger, N., & Ludwig, J. A. (2005). Linkages between microbial and hydrologic processes in arid and semiarid watersheds. *Ecology*, *86*, 298–307. https://doi.org/10.1890/03-0567

3. Bredehoeft, J. (1997). Safe yield and the water budget myth. *Ground Water*, *35*, 929–930.
4. Bredehoeft, J., Papadopoulos, S., & Cooper, H. (1982). The water budget myth (scientific basis of water management). *Studies in Geophysics, National Academy of Sciences*, *1*, 51–57.
5. Bredehoeft, J. D. (2002). The water budget myth revisited: Why hydrogeologists model. *Ground Water*, *40*, 340–345. https://doi.org/10.1111/j.1745-6584.2002.tb02511.x
6. Brunke, M., & Gonser, T. (1997). The ecological significance of exchange processes between rivers and groundwater. *Freshwater Biology*, *37*, 1–33. https://doi.org/10.1046/j.1365-2427.1997.00143.x
7. Brunner, P., Cook, P. G., & Simmons, C. T. (2009). Hydrogeologic controls on disconnection between surface water and groundwater. *Water Resources Research*, *45*, W01422. https://doi.org/10.1029/2008WR006953
8. Brunner, P., Cook, P. G., & Simmons, C. T. (2011). Disconnected surface water and groundwater: From theory to practice. *Ground Water*, *49*, 460–467. https://doi.org/10.1111/j.1745-6584.2010.00752.x
9. Brunner, P., Simmons, C. T., & Cook, P. G. (2009). Spatial and temporal aspects of the transition from connection to disconnection between rivers, lakes and groundwater. *Journal of Hydrology*, *376*, 159–169. https://doi.org/10.1016/j.jhydrol.2009.07.023
10. Carsel, R. F., & Parrish, R. S. (1988). Developing joint probability distributions of soil water retention characteristics. *Water Resources Research*, *24*, 755–769. https://doi.org/10.1029/WR024i005p00755
11. Cataldo, J., Behr, C., Montalto, F., & Pierce, R. J. (2004). A summary of published reports of transmission losses in ephemeral streams in the US. *National Center for Housing and the Environment*, *42*, 28–29.
12. Chui, T. F. M., & Freyberg, D. L. (2009). Implementing hydrologic boundary conditions in a multiphysics model. *Journal of Hydrologic Engineering*, *14*, 1374–1377. https://doi.org/10.1061/(ASCE)HE.1943-5584.0000113
13. Chui, T. F. M., Low, S. Y., & Liong, S.-Y. (2011). An ecohydrological model for studying groundwater–vegetation interactions in wetlands. *Journal of Hydrology*, *409*, 291–304. https://doi.org/10.1016/j.jhydrol.2011.08.039
14. Constantz, J., & Thomas, C. L. (1997). Stream bed temperature profiles as indicators of percolation characteristics beneath arroyos in the middle Rio Grande Basin USA. *Hydrological Processes*, *11*, 1621–1634. https://doi.org/10.1002/(SICI)1099-1085(19971015)11:12<1621::AID-HYP493>3.0.CO;2-X
15. Costa, A. C., Bronstert, A., & de Araújo, J. C. (2012). A channel transmission losses model for different dryland rivers. *Hydrology and Earth System Sciences*, *16*, 1111–1135. https://doi.org/10.5194/hess-16-1111-2012
16. Costigan, K. H., Kennard, M. J., Leigh, C., Sauquet, E., Datry, T., & Boulton, A. J. (2017). Chapter 2.2 flow regimes in intermittent Rivers and ephemeral streams. In *Intermittent rivers and ephemeral streams* (pp. 51–78). London, England: Academic Press.
17. Cuthbert, M. O., Acworth, R. I., Andersen, M. S., Larsen, J. R., McCallum, A. M., Rau, G. C., & Tellam, J. H. (2016). Understanding and quantifying focused, indirect groundwater recharge from ephemeral streams using water table fluctuations. *Water Resources Research*, *52*, 827–840. https://doi.org/10.1002/2015WR017503
18. Cuthbert, M. O., Gleeson, T., Moosdorf, N., Befus, K. M., Schneider, A., Hartmann, J., & Lehner, B. (2019). Global patterns and dynamics of climate–groundwater interactions. *Nature Climate Change*, *9*, 137–141. https://doi.org/10.1038/s41558-018-0386-4
19. Cuthbert, M. O., Taylor, R. G., Favreau, G., Todd, M. C., Shamsudduha, M., Villholth, K. G., … Kukuric, N. (2019). Observed controls on resilience of groundwater to climate variability in sub-Saharan Africa. *Nature*, *572*, 230–234. https://doi.org/10.1038/s41586-019-1441-7
20. Dahan, O., Tatarsky, B., Enzel, Y., Kulls, C., Seely, M., & Benito, G. (2008). Dynamics of flood water infiltration and ground water recharge in hyperarid desert. *Ground Water*, *46*, 450–461. https://doi.org/10.1111/j.1745-6584.2007.00414.x
21. Dai, A. (2012). Increasing drought under global warming in observations and models. *Nature Climate Change*, *3*(1), 52–58. https://doi.org/10.1038/nclimate1633
22. Decharme, B., Alkama, R., Douville, H., Becker, M., & Cazenave, A. (2010). Global evaluation of the ISBA-TRIP continental hydrological system. Part II: Uncertainties in river routing simulation related to flow velocity and groundwater storage. *Journal of Hydrometeorology*, *11*, 601–617. https://doi.org/10.1175/2010JHM1212.1
23. Döll, P., Douville, H., Güntner, A., Schmied, H. M., & Wada, Y. (2016). Modelling freshwater resources at the global scale: Challenges and prospects. In A. Cazenave, N. Champollion, J. Benveniste, & J. Chen (Eds.), *Remote sensing and water resources Space sciences series of ISSI* (pp. 5–31). New York, NY: Springer International Publishing.
24. Fan, Y., Li, H., & Miguez-Macho, G. (2013). Global patterns of groundwater table depth. *Science*, *339*, 940–943. https://doi.org/10.1126/science.1229881
25. Feng, S., & Fu, Q. (2013). Expansion of global drylands under a warming climate. *Atmospheric Chemistry and Physics*, *13*, 10081–10094. https://doi.org/10.5194/acp-13-10081-2013
26. Fox, G. A., & Durnford, D. S. (2003). Unsaturated hyporheic zone flow in stream/aquifer conjunctive systems. *Advances in Water Resources, Modeling Hyporheic Zone Processes*, *26*, 989–1000. https://doi.org/10.1016/S0309-1708(03)00087-3
27. Gleeson, T., Cuthbert, M., Ferguson, G., & Perrone, D. (2020). Global groundwater sustainability, resources and systems in the anthropocene. *Annual Review of Earth and Planetary Sciences*, *48*, 431–463. https://doi.org/10.1146/annurev-earth-071719-055251
28. GLP. (2005). *Science Plan and Implementation Strategy. (No. IGBP Report No. 53/IHDP Report No. 19)*. Stockholm: IGBP Secretariat.
29. Huang, J., Yu, H., Guan, X., Wang, G., & Guo, R. (2015). Accelerated dryland expansion under climate change. *Nature Climate Change*, *6*, 166–171. https://doi.org/10.1038/nclimate2837
30. IPCC. (2013). *Climate change 2013: The physical science basis: Working group i contribution to the fifth assessment report of the intergovernmental panel on climate change*. Cambridge, MA: Cambridge University Press.
31. Jaeger, K. L., Sutfin, N. A., Tooth, S., Michaelides, K., & Singer, M. (2017). Chapter 2.1:Geomorphology and sediment regimes of intermittent rivers and ephemeral streams. In T. Datry, N. Bonada, & A. Boulton (Eds.), *Intermittent rivers and ephemeral streams* (pp. 21–49). London, England: Academic Press. https://doi.org/10.1016/B978-0-12-803835-2.00002-4
32. Jarihani, A. A., Larsen, J. R., Callow, J. N., McVicar, T. R., & Johansen, K. (2015). Where does all the water go? Partitioning water transmission losses in a data-sparse, multi-channel and low-gradient dryland river system using modelling and remote sensing. *Journal of Hydrology*, *529*, 1511–1529. https://doi.org/10.1016/j.jhydrol.2015.08.030
33. Jazayeri-Shoushtari, S. M. H., Nielsen, P., Cartwright, N., & Perrochet, P. (2015). Periodic seepage face formation and water pressure distribution along a vertical boundary of an aquifer. *Journal of Hydrology*, *523*, 24–33.
34. Keppel, R. V., & Renard, K. G. (1962). Transmission losses in ephemeral stream beds. *Journal of the Hydraulics Division*, *88*, 59–68.
35. Knighton, A. D., & Nanson, G. C. (1994). Flow transmission along an arid zone anastomosing river, cooper creek, Australia. *Hydrological Processes*, *8*, 137–154. https://doi.org/10.1002/hyp.3360080205
36. Lerner, D., Issar, A., & Simmers, I. (1990). *Groundwater recharge: A guide to understanding and estimating natural recharge*, Hannover, Germany: Heise.
37. Malmon, D. V., Reneau, S. L., & Dunne, T. (2004). Sediment sorting and transport by flash floods. *Journal of Geophysical Research - Earth Surface*, *109*, 1–13. https://doi.org/10.1029/2003JF000067
38. McCallum, A. M., Andersen, M. S., Giambastiani, B. M. S., Kelly, B. F. J., & Ian Acworth, R. (2013). River-aquifer interactions in a

semi-arid environment stressed by groundwater abstraction: River-aquifer interactions in a semi-arid environment. *Hydrological Processes*, *27*, 1072–1085. https://doi.org/10.1002/hyp.9229
39. Meixner, T., Huth, A. K., Brooks, P. D., Conklin, M. H., Grimm, N. B., Bales, R. C., … Petti, J. R. (2007). Influence of shifting flow paths on nitrogen concentrations during monsoon floods, San Pedro River Arizona. *Journal of Geophysical Research: Biogeosciences*, *112*, 1–13. https://doi.org/10.1029/2006JG000266
40. Michaelides, K., Hollings, R., Singer, M. B., Nichols, M. H., & Nearing, M. A. (2018). Spatial and temporal analysis of hillslope–channel coupling and implications for the longitudinal profile in a dry-land basin. *Earth Surface Processes and Landforms*, *43*, 1608–1621. https://doi.org/10.1002/esp.4340
41. Peterson, D. M., & Wilson, J. L. (1988). *Variably saturated flow between streams and aquifers*, Las Cruces, NM: New Mexico Water Resources Research Institute-USGS.
42. Qin, D., Zhao, Z., Han, L., Qian, Y., Ou, L., Wu, Z., & Wang, M. (2012). Determination of groundwater recharge regime and flowpath in the lower Heihe River basin in an arid area of Northwest China by using environmental tracers: Implications for vegetation degradation in the Ejina Oasis. *Applied Geochemistry*, *27*, 1133–1145. https://doi.org/10.1016/j.apgeochem.2012.02.031
43. Rau, G. C., Halloran, L. J. S., Cuthbert, M. O., Andersen, M. S., Acworth, R. I., & Tellam, J. H. (2017). Characterising the dynamics of surface water-groundwater interactions in intermittent and ephemeral streams using streambed thermal signatures. *Advances in Water Resources*, *107*, 354–369. https://doi.org/10.1016/j.advwatres.2017.07.005
44. Renard, K. G., & Keppel, R. V. (1966). Hydrographs of ephemeral streams in the southwest. *Journal of the Hydraulics Division*, *92*, 33–52.
45. Reynolds, J. F., Smith, D. M. S., Lambin, E. F., Turner, B. L., Mortimore, M., Batterbury, S. P. J., … Walker, B. (2007). Global desertification: Building a science for Dryland development. *Science*, *316*, 847–851. https://doi.org/10.1126/science.1131634
46. Richards, L. A. (1931). Capillary conduction of liquids through porous mediums. *Physics*, *1*, 318–333. https://doi.org/10.1063/1.1745010
47. Sargeant, C. I., & Singer, M. B. (2016). Sub-annual variability in historical water source use by Mediterranean riparian trees. *Ecohydrology*, *9*, 1328–1345. https://doi.org/10.1002/eco.1730
48. Singer, M. B., Harrison, L. R., Donovan, P. M., Blum, J. D., & Marvin-DiPasquale, M. (2016). Hydrologic indicators of hot spots and hot moments of mercury methylation potential along river corridors. *Science of the Total Environment*, *568*, 697–711. https://doi.org/10.1016/j.scitotenv.2016.03.005
49. Singer, M. B., & Michaelides, K. (2014). How is topographic simplicity maintained in ephemeral dryland channels? *Geology*, *42*, 1091–1094. https://doi.org/10.1130/G36267.1
50. Singer, M. B., & Michaelides, K. (2017). Deciphering the expression of climate change within the lower Colorado River basin by stochastic simulation of convective rainfall. *Environmental Research Letters*, *12*, 104011. https://doi.org/10.1088/1748-9326/aa8e50
51. Snyder, K. A., & Williams, D. G. (2000). Water sources used by riparian trees varies among stream types on the San Pedro River Arizona. *Agricultural and Forest Meteorology*, *105*, 227–240. https://doi.org/10.1016/S0168-1923(00)00193-3
52. Sutfin, N. A., Shaw, J. R., Wohl, E. E., & Cooper, D. J. (2014). A geomorphic classification of ephemeral channels in a mountainous, arid region, southwestern Arizona, USA. *Geomorphology*, *221*, 164–175. https://doi.org/10.1016/j.geomorph.2014.06.005
53. Taylor, R. G., Scanlon, B., Döll, P., Rodell, M., Beek, R., Wada, Y., … Treidel, H. (2012). Ground water and climate change. *Nature Climate Change*, *3*(4), 322–329. https://doi.org/10.1038/nclimate1744
54. Theis, C. V. (1940). The source of water derived from wells. *Civil Engineering*, *10*, 277–280.
55. Trenberth, K. E., Dai, A., Schrier, G. van der, Jones, P. D., Barichivich, J., Briffa, K. R., & Sheffield, J. (2013). Global warming and changes in drought. *Nature Climate Change*, *4*, 12–22. https://doi.org/10.1038/nclimate2067
56. Valett, H. M., Fisher, S. G., & Stanley, E. H. (1990). Physical and chemical characteristics of the Hyporheic zone of a Sonoran Desert stream. *Journal of the North American Benthological Society*, *9*, 201–215. https://doi.org/10.2307/1467584
57. van Beek, L. P. H., & Bierkens, M. F. P. (2009). *The global hydrological model PCR-GLOBWB: Conceptualization, parameterization and verification (report)*. Utrecht, The Netherlands: Department of Physical Geography, Utrecht University.
58. van Genuchten, M. T. (1980). A closed-form equation for predicting the hydraulic conductivity of unsaturated Soils1. *Soil Science Society of America Journal*, *44*, 892–898. https://doi.org/10.2136/sssaj1980.03615995004400050002x
59. Vivoni, E. R., Bowman, R. S., Wyckoff, R. L., Jakubowski, R. T., & Richards, K. E. (2006). Analysis of a monsoon flood event in an ephemeral tributary and its downstream hydrologic effects. *Water Resources Research*, *42*, 1–11. https://doi.org/10.1029/2005WR004036
60. Wada, Y., van Beek, L. P. H., van Kempen, C. M., Reckman, J. W. T. M., Vasak, S., & Bierkens, M. F. P. (2010). Global depletion of groundwater resources. *Geophysical Research Letters*, *37*, L20402. https://doi.org/10.1029/2010GL044571
61. Wada, Y., Wisser, D., & Bierkens, M. F. P. (2014). Global modeling of withdrawal, allocation and consumptive use of surface water and groundwater resources. *Earth System Dynamics*, *5*, 15–40. https://doi.org/10.5194/esd-5-15-2014
62. Wang, P., Pozdniakov, S. P., & Vasilevskiy, P. Y. (2017). Estimating groundwater-ephemeral stream exchange in hyper-arid environments: Field experiments and numerical simulations. *Journal of Hydrology*, *555*, 68–79. https://doi.org/10.1016/j.jhydrol.2017.10.004
63. Wang, P., Yu, J., Pozdniakov, S. P., Grinevsky, S. O., & Liu, C. (2014). Shallow groundwater dynamics and its driving forces in extremely arid areas: A case study of the lower Heihe River in northwestern China. *Hydrological Processes*, *28*, 1539–1553. https://doi.org/10.1002/hyp.9682
64. Wang, W., Dai, Z., Zhao, Y., Li, J., Duan, L., Wang, Z., & Zhu, L. (2016). A quantitative analysis of hydraulic interaction processes in stream-aquifer systems. *Scientific Reports*, *6*, 19876. https://doi.org/10.1038/srep19876
65. Wheater, H., Sorooshian, S., & Sharma, I. K. D. (2008). *Hydrological Modelling in arid and semi-arid areas*. Cambridge, MA: Cambridge University Press.
66. Winter, T. C. (1995). Recent advances in understanding the interaction of groundwater and surface water. *Reviews of Geophysics*, *33*, 985–994. https://doi.org/10.1029/95RG00115
67. Winter, T. C., Harvey, J. W., Franke, O. L., & Alley, W. M. (1998). *Circular: Ground water and surface water; a single resource*, Reston, VA: USGS Numbered Series No. 1139. U.S. Geological Survey.
68. Xian, Y., Jin, M., Liu, Y., & Si, A. (2017). Impact of lateral flow on the transition from connected to disconnected stream–aquifer systems. *Journal of Hydrology*, *548*, 353–367. https://doi.org/10.1016/j.jhydrol.2017.03.011
69. Xie, Y., Cook, P. G., Brunner, P., Irvine, D. J., & Simmons, C. T. (2014). When can inverted water tables occur beneath streams? *Groundwater*, *52*, 769–774. https://doi.org/10.1111/gwat.12109

How to cite this article: EA Quichimbo, MB Singer, MO Cuthbert. Characterising groundwater–surface water interactions in idealised ephemeral stream systems. *Hydrological Processes*. 2020;1–15. https://doi.org/10.1002/hyp.13847